



STRUCTURAL AND MORPHOLOGICAL INVESTIGATIONS OF SULFUR BASED CATHODE FOR LITHIUM SULFUR BATTERIES

¹G. Radhika, ¹K. Krishnaveni, ¹R. Subadevi, ¹M. Sivakumar

¹School of Physics, Alagappa University, Karaikudi-630 004. Tamil Nadu, India.

ABSTRACT- The Lithium–sulfur battery (Li–S battery) is a type of rechargeable battery, notable for its high energy density. Lithium–sulfur batteries may succeed lithium-ion cells because of their higher energy density and reduced cost from the use of sulfur. Lithium sulfur batteries with a higher theoretical capacity of 1672 mAhg^{-1} than commercial LIB systems can meet these requirements. A simple and facile synthesis route for S/PvdF/TiO₂ composite via solid state reaction. The composite material has been characterized by XRD, FTIR and RAMAN Analysis. The SEM was carried out in detail to study the surface morphology and it reveals that the sulfur is uniformly dispersed in the TiO₂ matrix. From the above investigation, the composite is a favourable cathode material for lithium sulfur batteries.

Keywords-[Lithium-sulfur battery, cathode, composite, TiO₂]

1. INTRODUCTION

The rapid development of emerging applications, including military power supplies, civil transportation, and stationary storage, placed higher demands on the energy density of the battery, which resulted in the resurgent of Li-S batteries. The Li–S battery works on the basis of redox reactions between a lithium metal anode and a sulfur cathode. The combination of lithium metal with a theoretical specific capacity of 3830 mAhg^{-1} as the anode and elemental sulfur (S) with a theoretical specific capacity of 1675 mAhg^{-1} as the cathode in a battery can generate a high theoretical specific energy of 2600 Whkg^{-1} [1–4] and is up to five times greater than that of commercial LIBs (387 Whkg^{-1} for LiCoO₂/C battery). The practical energy

density of packaged Li-S batteries could be as high as 400 to 600 Whkg^{-1} (two or three times higher than that of commercial LIBs). Furthermore, the abundance and non-toxicity of S provide Li-S batteries with improved energy economy and environmental friendliness. In addition, sulfur is abundant and inexpensive. However, the practical usage of sulfur as the cathode for lithium rechargeable has not been successful yet which attributed to several reasons. Lithium polysulfides are intermediate products of electrochemical reactions between sulfur and lithium ions. They dissolve in liquid ether-based electrolyte easily, which leads to loss of sulfur species.[5,6] In the process of charge, dissolved high-order lithium polysulfides diffuse through the separator to the lithium

electrode. They react with lithium and are deoxidized to low-order lithium polysulfides which migrate to the sulfur electrode and are oxidized to high order lithium polysulfides. Repetition of those processes results in low coulombic efficiency.[7,8] The agglomeration for sulfur species in the sulfur electrode causes the low cycling capacity. In the process of discharge, dissolved lithium polysulfides are deoxidized to insoluble lithium bisulfide and lithium sulfide. They precipitate on the surface of the sulfur electrode. [9] The cyclic precipitation causes agglomeration for sulfur species[10] and separation between sulfur species and electrically conductive substances. Therefore, Li-S batteries show great potential for the next generation of lithium batteries and are capable of offering high energy density power sources for electric vehicles. [11]

2. EXPERIMENTAL WORK

The STFA composite was synthesized by solid state method. The TiO_2 mixed with PvdF powder in definite ratio and then heated to 200°C for 3h and then mixed with sulfur heated at 155°C for 20h. The final product is denoted as STFA composite. The structural, functional groups and morphology were investigated by XRD, FTIR, RAMAN and SEM.

3. CHARACTERISATION OF MATERIALS

Morphology and structure of materials were characterized by Scanning electron microscopy (FEG Quanta 250) and X-ray diffraction (PANalytical X'pertPro Powder X-ray diffraction). Chemical bonds of substances were characterized by Fourier transform infrared spectroscopy (Thermo Nicolet 380 FTIR Spectrophotometer) and Raman spectroscopy (SEKI focal).

4. RESULTS AND DISCUSSION

A. X-RAY Diffractometer

The XRD patterns of pure sulfur, TiO_2 and STFA composite are present in fig. 1. Sulfur showed typical orthorhombic sulfur

crystalline diffraction peaks with (jcpds no:24-0733). In the X-ray diffraction Patterns of TiO_2 is the rutile structure confirmed with (jcpds no:65-190). As for STFA there is no any new phase in the final product except pure sulfur and rutile miscrystal. The good dispersion of sulfur in the STFA composite does not change the crystal structure of pure sulfur and rutile TiO_2 composite.[12]

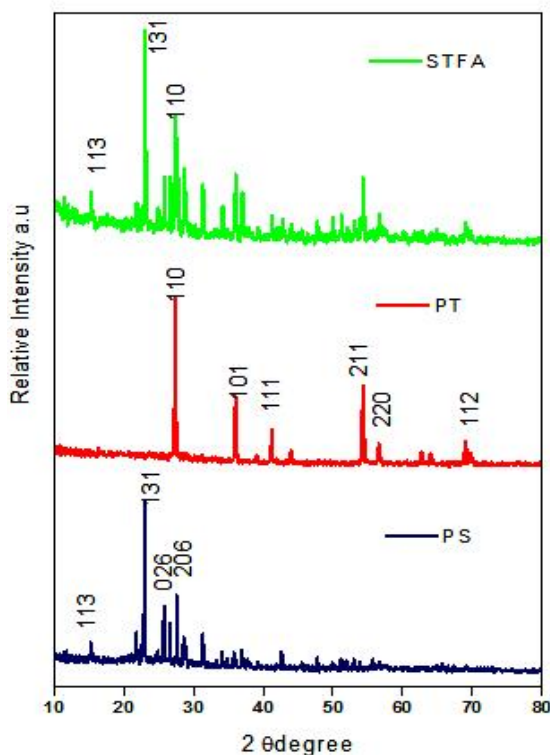


Figure 1- XRD Pattern of Pure sulfur (PS), Pure TiO_2 (PT) and STFA composite

B. FOURIER TRANSFORM INFRARED SPECTROSCOPY

Fourier Transform Infrared Spectroscopy (FTIR) offers quantitative and qualitative analysis for organic and inorganic samples. FTIR identifies chemical bonds in a molecule by producing an infrared absorption spectrum. FTIR is an effective analytical instrument for detecting functional groups and characterizing covalent bonding information. In STFA composite show the peaks corresponding to stretching vibrations of O-H and bending vibrations of adsorbed water molecules around $3300\text{--}3500\text{ cm}^{-1}$. The peak around 1642 cm^{-1} corresponds to the --C=C-- stretch vibration. Also, the peak at 513 cm^{-1} should assign to the stretching

vibration of Ti-O is shown in fig 2. Peak around 878 cm^{-1} indicates CF_2 asymmetric stretching mode [13]

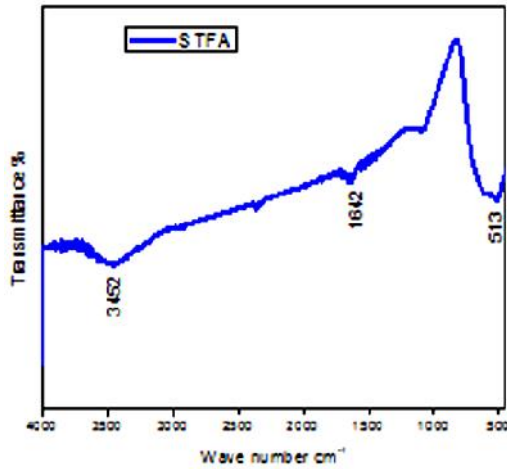


Figure 2- FTIR spectra for STFA composite

C. MICRORAMAN SPECTROSCOPY

Raman spectroscopy is a spectroscopic technique used to observe vibrational, rotational, and other low-frequency modes in a system. [14] Raman spectra of STFA composite were shown the Fig.3. The Raman shifts of Rutile crystal dominant peaks are appeared at 140, 235, 445, 609 and 825 cm^{-1} . The observed Raman shifts are shifted to 160, 240, 440.9, 608.8 cm^{-1} respectively [15].

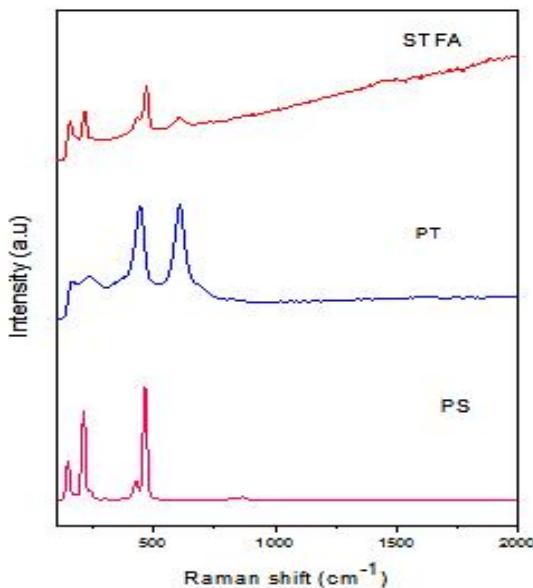


Figure 3- RAMAN spectra for Pure sulfur (PS), Pure TiO_2 (PT) and STFA composite

D. SCANNING ELECTRON MICROSCOPY

The Fig.4. shows the morphology of the STFA composite.. The surface of STFA composite seems to be smoother, which could be due to the sulfur coating. However, agglomeration or particles of sulfur are not observed in the STFA composite.

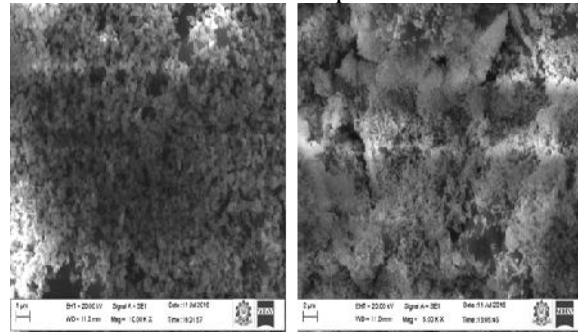


Figure 4- SEM image of STFA composite

CONCLUSION

In this work, STFA composite material was successfully synthesized by a solid state reaction method. The powder XRD pattern of pristine sulfur exhibited orthorhombic structure with Fddd space group. The diffraction peaks with reduced intensity indicate that the sulfur is fully incorporated into the pores of coating material. The enhanced performances of STFA composite cathode material attributed to the good dispersion of sulfur into the TiO_2 particles and may adsorb lithium polysulfides by TiO_2 . The strategy of developing a structure by incorporating the merits of TiO_2 has great advantages and can feasible way to improve the performance of other electrode materials in Lithium Ion batteries.

REFERENCES

- [1]. R. D. Rauh, K. M. Abraham, G. F. Pearson, J. K. Surprenant and S. B. Brummer, J. Electrochem. Soc., 1979, 126, 523.
- [2]. J. Shim, K. A. Striebel and E. J. Cairns, J. Electrochem. Soc., 2002, 149, A1321.
- [3]. D. Peramunage and S. Licht, Science, 1993, 261, 1029.

- [4]. J. Wang, S. Y. Chew, Z. W. Zhao, S. Ashraf, D. Wexler, J. Chen, S. H. Ng, S. L. Chou and H.K. Liu, *Carbon*, 2008, 46, 229.
- [5]. J. X. Song, Z. X. Yu, T. Xu, S. R. Chen, H. Sohn, M. Regula and D. H. Wang, *J. Mater. Chem. A*, 2014, 2, 8623.
- [6]. Q. Li, Z. A. Zhang, Z. P. Guo, K. Zhang, Y. Q. Lai and J. Li, *J. Power Sources*, 2015, 274, 338.
- [7]. C. X. Zu, Y. Z. Fu and A. Manthiram, *J. Mater. Chem. A*, 2013, 1, 10362.
- [8]. C. Wang, W. Wan, J. T. Chen, H. H. Zhou, X. X. Zhang, L. X. Yuan and Y. H. Huang, *J. Mater. Chem. A*, 2013, 1, 1716.
- [9]. B. Ding, C. Z. Yuan, L. F. Shen, G. Y. Xu, P. Nie, Q. X. Lai and X. G. Zhang, *J. Mater. Chem. A*, 2013, 1, 1096.
- [10]. C. N. Lin, W. C. Chen, Y. F. Song, C. C. Wang, L. D. Tsai and N. L. Wu, *J. Power Sources*, 2014, 263, 98.
- [11]. Yu-Guo Guo and Li-Jun Wan, *Electrochemistry, Materials, and Prospects*, DOI: 10.1002/anie.201304762
- [12]. Xin Zhou Ma, Bo Jin, Hui Yuan Wang, Jia Zi Hou, Xiao Bin Zhong, Huan Huan Wang, Pei Ming Xin-*Journal of Electroanalytical Chemistry* S1572-6657(14)00492-5.
- [13]. Sang-Hun Nam, Tae Kwan Kim, Jin-Hyo Boo-*Catalysis Today* 185 (2012) 259– 262
- [14]. Gardiner, D.J. (1989). *Practical Raman spectroscopy*, Springer-Verlag ISBN 978-0-387-50254-0.
- [15]. H.L. Ma , J.Y. Yang, Y. Dai, Y.B. Zhang, B. Lu, G.H. Ma-*Applied Surface Science* 253 (2007) 7497–7500.